RDX AND HMX FLAME STRUCTURE AT A PRESSURE OF 0.1 MPa

Evgeny N. Volkov,[1] Alexander A. Paletsky,[1] and Oleg P. Korobeinichev[1,2]
[1]*Institute of Chemical Kinetics and Combustion SB RAS, Novosibirsk, Russia*
[2]*Novosibirsk State University, Russia*

ABSTRACT

The chemical flame structure of cyclic nitramines (HMX, RDX) was investigated at a pressure of 0.1 MPa using molecular beam mass spectrometry. HMX and RDX strands were burned in air and argon atmosphere, respectively. It was obtained that at atmospheric pressure combustion of HMX (unlike to RDX) is unstable. Eleven species (H_2, H_2O, HCN, CO_2, CO, N_2, N_2O, CH_2O, NO, NO_2 and nitramine vapor (HMX or RDX)) were found in flames of HMX and RDX during its self-sustained combustion at a pressure of 0.1 MPa. It was found that nitramine flame at a pressure of 0.1 MPa has a two-zone structure. In the first flame zone, the consumption of nitramine vapor (HMX or RDX), NO_2, CH_2O and partial consumption of N_2O with formation of H_2, H_2O, CO, N_2, CO_2, HCN and NO occurs. In the second flame zone, the main reaction is oxidation of HCN by NO accompanied with formation of final combustion products. Using experimental data, brutto-reactions for the gasification of nitramines at atmospheric pressure were determined. Data obtained in this work can be used for further development of the mechanism of gas-phase chemical reactions occurring in RDX and HMX flames.

INTRODUCTION

Cyclic nitramines, such as RDX and HMX, are well-known energetic materials (EM). Numerous experimental and theoretical investigations have been devoted to the study of combustion characteristics of RDX and HMX. Experimental investigations of their chemical flame structure were conducted at different pressures (from 0.02 to 0.2 MPa) during self-sustained and laser-assisted combustion.[1–6] Experimental methods used for studying chemical flame structure of RDX and HMX include probe mass-spectrometry and optical spectroscopic methods, such as planar laser-induced fluorescence (PLIF) and UV-vis absorption spectroscopy. However, the research is still insufficient. Combustion models assume the presence of nitramine vapor in gas phase;[7]

however, available experimental data cannot confirm or deny its presence in the flame. The main goal of the present work was to study chemical flame structure of cyclic nitramines (RDX and HMX) during their self-sustained combustion at a pressure of 0.1 MPa. Much attention was given to the determination of product composition near the burning surface–especially to identifying nitramine vapor and measuring its concentrations, and also to determining the brutto-reaction for gasification of nitramines in a combustion wave using experimental data.

EXPERIMENTAL TECHNIQUE

Experiments on combustion of RDX and HMX were conducted in a combustion chamber at a pressure of 0.1 MPa. The pressed strands of nitramines were 8 mm in diameter and 6–8 mm in height. The density of RDX and HMX strands was equal to 1.7 g/cm^3 and 1.8 g/cm^3, respectively. The structure of RDX and HMX flames was studied using the molecular beam mass spectrometric (MBMS) system based on a time-of-flight mass spectrometer. Combustion products were sampled from flame using an aluminum "sonic" probe with a thin layer of Al_2O_3 on the surface. The opening angle of the internal cone of the probes was equal to ~ 40°. Wall thickness of the probe and diameter of inlet orifice were equal to ~ 70 microns. Identification of combustion products was conducted using calibration mass spectra and calibration coefficients were utilized in determining their concentrations. Final flame temperature of RDX was measured using WRe (5%)–WRe (20%) thermocouple of 50 microns in diameter.

RESULTS AND DISCUSSION

Investigation of self-sustained combustion of RDX and HMX at a pressure of 0.1 MPa is somewhat complicated because of their combustion behavior at this pressure. During the ignition of RDX strands (in argon) at a pressure of 0.1 MPa, the formation of big bubbles was observed in all experiments on the surface of strands. In some experiments, these bubbles completely disappeared after the ignition, and in others, they remained on the strand surface during the combustion. When bubbles were present on the burning surface, combustion of RDX strands was unstable and even ceased several seconds after the ignition (incomplete burning of the strand). In a significant number of cases (~ 40% of all experiments), a stable combustion (without bubbles) with a burning rate of ~ 0.27 mm/s was observed. So RDX can burn stably in an inert atmosphere at a pressure of 0.1 MPa. HMX strands could not be ignited in an inert atmosphere. In an atmosphere of air, HMX strands could sustain combustion, but it was unstable (with variable burning rate). The average burning rate of HMX strands was equal to ~ 0.65 mm/s. Unstable combustion of HMX was also observed in Parr et al.[2] and Simonenko et al.[8]

The value of final flame temperature of RDX, measured at a distance of ~ 3 mm from the burning surface, was equal to ~ 2800 K with a correction for thermocouple radiation. The thermocouple could withstand RDX flame without destruction only for ~ 0.9 s. The obtained value of the final flame temperature of RDX at atmospheric pressure is in agreement with that measured using optical spectroscopy.[2]

Chemical Flame Structure of RDX and HMX at a Pressure of 0.1 MPa

In flames of RDX and HMX, the following species: H_2 (2), H_2O (18, 17), HCN (27, 26, 14), CO (28, 12), N_2 (28, 14), CH_2O (29, 30), NO (30, 14), CO_2 (44, 28, 22), N_2O (44, 30, 28, 14), NO_2 (46, 30, 14) and corresponding nitramine vapor (75, 46, 42, 30, 29) were identified and their concentration profiles were measured. The mass peaks used for interpretation of mass spectra, obtained during probing of nitramine flames, are shown in parentheses. These species (with the exception of nitramine vapor) were also found in nitramine flames during laser-assisted combustion.[3,6] In addition to the above-mentioned peaks, other mass of lower density peaks were also found. In the case of RDX, Mass Peaks 43 and 42, which can probably be attributed to HNCO or HCNO, should be mentioned. In the case of HMX, the number of these mass peaks is significantly higher (brutto-formulas of probable species are shown in parentheses): 40, 41, 42 and 43 (HNCO or HCNO), 45 (H_3NCO), 47 (HNO_2), 52 (C_2N_2), 54 ($C_2H_2N_2$), 67, 70 (H_2C_2NO), 81 ($H_3C_3N_3$). Mass Peaks 40, 41 and 67 were not identified. Preliminary identified mass peaks have not been taken into account in the calculations of flame structure.

The flame structure of RDX at a pressure of 0.1 MPa is shown in Fig. 1. Considering the behavior of mole fraction profiles, species can be separated into three groups: 1) species, which are completely consumed at a distance of ~ 0.3 mm from the burning surface (RDX_v, NO_2, N_2O, CH_2O); 2) species with wider zone of consumption (HCN, NO); and 3) final combustion products, the mole fraction of which monotonically increases (N_2, CO, H_2O, H_2, CO_2).

In order to check the correctness of determined species concentrations, a content of elements at different distances from the burning surface was calculated. Element content profiles in RDX flame, calculated while ignoring the diffusion fluxes of species, are presented in Fig. 1. One can see that the calculated content of elements coincides with good accuracy with initial element content in RDX. Mass fraction of RDX vapor on the burning surface is equal to ~ 40%. About 85% of RDX vapor decompose narrowly, adjacent to the burning surface flame zone with width of ~ 0.15 mm. Mass fractions of N_2O, CH_2O and NO_2 also decrease in this zone (by ~ 2 times). This leads to formation of NO, HCN, N_2, CO, CO_2, H_2O and H_2. Complete consumption of N_2O, CH_2O and NO_2 occurs only at a distance of ~ 0.3 mm. In the end of

narrow flame zone with width of ~ 0.15 mm, mass fractions of HCN and NO reach their maximum values and the second zone (the zone of oxidation of HCN by NO with formation of final combustion products) begins. Complete consumption of HCN occurs only at a distance of ~ 1 mm. Consumption of NO is not complete even at a distance of ~ 2 mm.

With the exception of NO, the composition of final combustion products is close to thermodynamically equilibrium composition (Table 1), calculated using "Astra" code.[9] High value of NO mole fraction (0.05) in final combustion products indicates that completeness of combustion was not achieved.

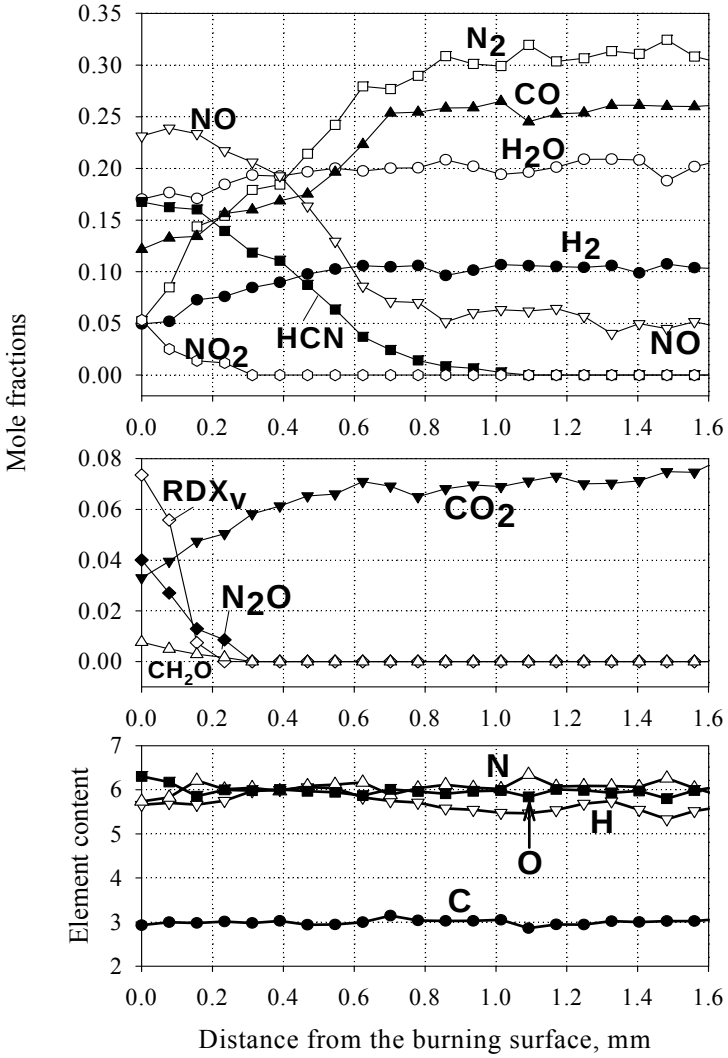

Figure 1: RDX flame structure at a pressure of 0.1 MPa (in Ar)

The profile of NO concentration in an RDX flame at a pressure of 0.1 MPa, measured using optical spectroscopy, is characterized by significant scatter;[10] nevertheless, it is in qualitative agreement with that measured in our work using molecular beam mass spectrometry. Moreover, at a distance from ~ 0.04 to 0.3 mm, where the value of NO mole fraction is maximum and scatter of data (obtained using optical spectroscopy), is minimum, these two profiles are in good agreement.

The two-zone flame structure of RDX, determined by concentration profiles, is in agreement with data on temperature profiles.[2,11] The width of the first zone (~ 0.15 mm) satisfactorily coincides with the point location on temperature profiles (0.1–0.12 mm), in which a significant decrease of temperature gradient (by ~ 2 times) takes place. The second zone ends at a distance of ~ 1 mm from the burning surface – considerable slowing of temperature growth on the temperature profile is observed approximately at the same distance. These data together can be used for validation of RDX combustion mechanism.

Figures 2a and 2b show species concentration profiles in HMX flame for self-sustained combustion in an air atmosphere at a pressure of 0.1 MPa. The *x* axis in Fig. 2a is a relative time corresponding to "movement of the probe away from the burning surface." It can be seen that pulsations are present on concentration profiles. Duration of these pulsations comprises 0.3–0.5 s, and a frequency of their appearance is equal to ~ 0.7 Hz. The first pulsation exhibits itself mostly as an increase in N_2O concentration at 0.7–0.9 s. Three more pulsations (from 2 to 5 s) relate to the simultaneous increase of HCN and NO concentrations and decrease of CO and N_2 concentrations. Analysis of video recording showed that at $t > 2.7$ s, the tip of the probe was situated in a luminous flame zone. However, at the moments of time corresponding to appearance of pulsations (observed at $t > 2.7$ s), decrease in flame luminosity under the probe took place. Concentrations of HCN, NO, CO and N_2 at these moments of time also correspond to those in dark flame zone. Analysis of video recordings showed that at these moments of time, an increase of burning rate from ~ 0.45 mm/s (at the period of time from 2.7 to 3.7 s) to ~ 0.8 mm/s occurred, which led to a temporary increase in width of the flame zone and, as a result, a temporary increase in the appearance of these pulsations on the concentration profiles. It should be noted that significant change (during the pulsations) in concentrations of some species (up to 30% from maximal value) did not affect the content of elements in the flame zone (Fig. 2a).

Smoothed, distance-dependent profiles of species concentration in HMX flame are presented in Fig. 2b. The distance from the burning surface was calculated using an average value of velocity for the movement of the burning surface towards the probe equal to ~ 0.6 mm/s.

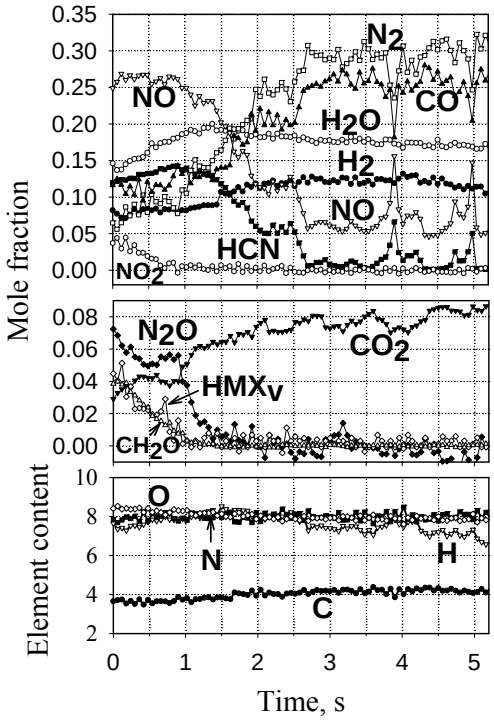

Figure 2a: HMX flame structure at a pressure of 0.1 MPa (in air), time-dependent profile

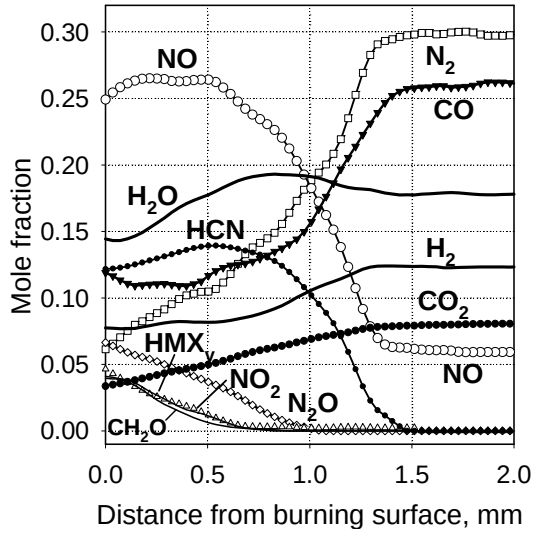

Figure 2b: HMX flame structure at a pressure of 0.1 MPa (in air), smoothed, distance-dependent profiles

The HMX flame at a pressure of 0.1 MPa also has a two-zone structure. In the first zone with a width of ~ 0.7 mm, consumption of HMX vapor, NO_2, CH_2O, and partial consumption of N_2O with formation of H_2, H_2O, CO, N_2, CO_2, HCN and NO occur. The zone of complete consumption of N_2O exceeds the zone of consumption of HMX vapor (as in the RDX flame). In the second flame zone, at a distance of 0.7–1.5 mm from the burning surface, consumption of HCN and NO with formation of final combustion products takes place.

A detailed mechanism of chemical reactions, including initial steps of RDX vapor decomposition, was proposed by Melius,[12] which was later supplemented and improved by Yetter et al.[13] The latter served as the basis for many subsequent combustion models of RDX.[10,14–16] The comparison of results from modeling RDX flame structure,[10,17] obtained here in experimental data, shows that, in general, RDX combustion models satisfactorily describe its flame structure for self-sustained combustion at a pressure of 0.1 MPa. There is good agreement with concentration profiles for most of the main combustion products. For better future agreement, a further improvement of combustion models is needed, containing a more accurate description of processes in the condensed phase as well as a more precise definition of rate constants in chemical reactions.

Analysis of Composition of Final Combustion Products

In Table 1, compositions of final combustion products of RDX and HMX are presented. Content of elements in final combustion products of RDX ($C_{2.97}H_{5.55}O_{5.93}N_{6.13}$) and HMX ($C_{4.13}H_{7.31}O_{7.98}N_{7.96}$) is close to initial element compositions of RDX ($C_3H_6O_6N_6$) and HMX ($C_4H_8O_8N_8$). Maximal deviation from initial content is observed for H and comprises 7.5% and 8.6% for RDX and HMX, respectively. A shortage of H in measured compositions of final combustion products is mainly caused by an absence of H and OH radicals in these compositions. Concentrations of H and OH radicals were not measured in our experiments; however, thermodynamic equilibrium composition contains these radicals in rather high concentrations. In order to calculate temperature so that it measures the corresponding composition of the final combustion products, it is necessary to add the H and OH radicals. Earlier it was demonstrated that the concentration of the OH radical in the final combustion products of RDX during its self-sustained combustion at a pressure of 0.1 MPa is close to equilibrium concentration.[2,10] In the case of HMX, the experimentally-measured mole fraction of OH radical $(0.036)^2$ is higher than equilibrium value (0.026). This difference is most likely caused by measurement error. Therefore, in the first approximation, both measured compositions of final combustion products were modified so that the concentrations of H and OH radicals coincided with those in equilibrium compositions. The modified compositions of final combustion products are also presented in Table 1. Such modification led to the improvement of overall element balance: RDX - $C_{2.91}H_{6.04}O_{6.06}N_{6.01,}$ HMX - $C_{4.04}H_{7.97}O_{8.15}N_{7.79}$.

Table 1: Composition of final combustion products (in mole fractions) in RDX and HMX flames at a pressure of 0.1 MPa in comparison with thermodynamically equilibrium composition

	H_2	H_2O	N_2	CO	NO	CO_2	H	OH
RDX, experiment	0.104	0.202	0.312	0.256	0.053	0.072	– *	– *
HMX, experiment	0.123	0.178	0.298	0.260	0.060	0.080	– *	– *
RDX, equilibrium**	0.090	0.195	0.315	0.245	0.005	0.073	0.038	0.026
HMX, equilibrium **	0.089	0.196	0.316	0.244	0.005	0.073	0.038	0.026
RDX, modified	0.098	0.189	0.292	0.240	0.049	0.068	0.038	0.026
HMX, modified	0.115	0.167	0.279	0.244	0.056	0.075	0.038	0.026

*Concentrations of H and OH radicals were not measured.
**Thermodynamical equilibrium composition was calculated using "Astra" code;[9] species with mole fraction less than 0.01 are not shown in this table.

Brutto-reactions of transformation of RDX and HMX in final combustion products (Nitramine $\rightarrow \Sigma\alpha_i A_i$) on the basis of modified compositions can be written as:

$$\text{RDX} \rightarrow 2.77\ N_2 + 2.27\ CO + 1.79\ H_2O + 0.93\ H_2 + 0.64\ CO_2 + 0.47\ NO + \\ + 0.36\ H + 0.25\ OH \quad (1)$$

$$\text{HMX} \rightarrow 3.54\ N_2 + 3.09\ CO + 2.12\ H_2O + 1.46\ H_2 + 0.95\ CO_2 + 0.71\ NO + \\ + 0.48\ H + 0.33\ OH \quad (2)$$

Heat release, Q, in reactions (1) and (2) was determined as:

$$Q = -\Delta H = \Delta_f H^o_{solid}(\text{Nitramine}) - \Sigma\alpha_i \cdot \Delta_f H^o(A_i) \quad (3)$$

Calculations showed that the heat release in these reactions [Eqs. (1) and (2)] comprise 955 and 1227 kJ per 1 mole of RDX and HMX, respectively. Enthalpies for the formation of solid RDX (71.1 kJ/mole) and HMX (87.9 kJ/mole) were taken from Krien et al.,[18] and enthalpies for formation of other compounds, from the NIST database.[19]

The temperature for the products of reactions in Eqs. (1) and (2), i.e., temperature of final combustion products, T_f, was estimated using the formula:

$$Q = \alpha(H_2O) \cdot \Delta H_{vap}(H_2O, 298\,K) + \int_{298\,K}^{T} c_{p,\,mixture}(T)\,dT \quad (4)$$

Calculations showed that modified compositions of the final combustion products of RDX and HMX correspond to 2775 and 2710 K, respectively. In

both cases, the calculated temperatures were less than the corresponding adiabatic temperatures (T_{ad} (RDX) = 2929 K, T_{ad} (HMX) = 2925 K). In the case of RDX, calculated temperature was in good agreement with that of the final combustion products equal to ~ 2800 K measured by us. In the case of HMX, calculated temperature was higher by ~ 320 K than the value measured using tungsten-rhenium thermocouples,[20,21] and lower by 190 K than the value measured using optical spectroscopy.[22]

Reaction of Gasification and Heat Release in the Reaction Layer of the Condensed Phase

Stoichiometric coefficients (ν_i) of the brutto-reaction for gasification of nitramines (Nitramine $\rightarrow \Sigma\nu_i B_i$) can be calculated from the mass fluxes of products near the burning surface. The stoichiometric coefficient of each product is defined as a ratio of mass flux of each on the burning surface to the mass flux of nitramine. Non-dimensional mass fluxes of products (G_i) taking into account of species diffusion and thermo diffusion can be written as follows:

$$G_i = \frac{M_i}{M}\left(x_i - \frac{D_{im}}{v}\cdot\frac{dx_i}{dz}\right) - \frac{1}{\rho\cdot v}\cdot\frac{D_i^T}{T}\cdot\frac{dT}{dz} \qquad (5)$$

where x_i = mole fraction of B_i species; dx_i/dz = gradient of concentration of B_i species; M_i = molecular weight of B_i species; M = average molecular weight; ρ = density; v = velocity of species flux; T = temperature; dT/dz = temperature gradient; D_{im} = mixture diffusion coefficient of B_i species; and D_i^T = thermo-diffusion coefficient of B_i species.

In Table 2, experimentally measured compositions of products near the burning surface of RDX and HMX at a pressure of 0.1 MPa are presented. Comparison of the compositions showed that they are quite close to each other. In the case of HMX concentration of CH_2O near the burning surface is higher than in the case of RDX, and HCN concentration is lower. The concentration of N_2O, which is formed by the same decomposition pathway of HMX and RDX as CH_2O,[23] is also higher in the case of HMX. Whereas the concentration of NO_2, which is formed by the same decomposition pathway as HCN,[23] is lower in the case of HMX.

In order to calculate mass fluxes of products on the burning surface, it is necessary to know the temperature of the burning surface and the temperature gradient in the gas phase near the burning surface. The temperature of the burning surface (T_s) of RDX at a pressure of 0.1 MPa was measured to be equal to 593[11] and 605 K.[2] In calculations, the mean value of 600 K was used. The value of the temperature gradient near the burning surface ($8–10^6$ K/m) was taken from Zenin.[11] In another instance, the experimental work value of the temperature gradient differs by 25%;[21] however this difference lies within the

limits of measurement error related to such a high temperature gradient. Calculations of brutto-reaction for gasification of HMX at a pressure of 0.1 MPa were conducted for three values of T_s and the corresponding values of temperature gradient: T_s = 687 K, $dT/dx=3.55\cdot10^6$ K/m,[24] T_s = 633 K, $dT/dx=4\cdot10^6$ K/m,[11] and T_s = 593 K, $dT/dx=7\cdot10^6$ K/m.[20] In the case of HMX, the gradients of species concentrations, determined using smoothed concentration profiles (Fig. 2b), were used in these calculations.

Table 2: Compositions (in mole fractions) of products near the burning surface and gasification products of RDX and HMX at a pressure of 0.1 MPa

	RDX *	RDX **	HMX *	HMX **
H_2	0.049	0.105	0.077	0.099
H_2O	0.170	0.162	0.144	0.145
HCN	0.168	0.166	0.122	0.119
N_2	0.052	0.009	0.061	0.055
CO	0.122	0.108	0.119	0.121
CH_2O	0.008	0.010	0.040	0.039
NO	0.231	0.220	0.249	0.238
CO_2	0.033	0.024	0.034	0.032
N_2O	0.040	0.049	0.066	0.067
NO_2	0.053	0.079	0.041	0.041
RDX_v/HMX_v	0.074	0.067	0.047	0.045
C:H:O:N	2.93:5.66:6.30:5.74	2.86:6.30:6.50:5.53	3.72:7.56:8.48:7.73	3.74:7.98:8.50:7.65

*Experimentally measured composition of products near the burning surface
**Composition of gasification products

Table 2 also shows the compositions of gasification products of RDX and HMX–concentrations of species in a flux from the burning surface to the gas phase. The composition of HMX gasification products presented in this table corresponds to T_s = 633 K and $dT/dx=4\cdot10^6$ K/m.[11] The use of a higher value of temperature gradient near the burning surface of RDX (10^7 K/m)[21] results in a small variation of the composition of gasification products. In the case of HMX, concentrations of products near the burning surface change slightly; therefore, changes of product composition, caused on account of diffusion, are not very significant. An accounting of thermodiffusion causes significant influence only on the concentration of H_2, which has the lowest molecular weight among the products near the burning surface. In addition to H_2, a noticeable change in the absolute value of concentration is observed for NO, which is caused by its high concentration of NO. Calculations for strongly different temperatures of the burning surface (593 and 687 K), but with the same temperature gradient, showed that calculated compositions are almost

identical. It means that, in this case, the existing scatter in the values of temperature for the burning surface does not significantly influence the result of calculation for the composition of gasification products. The existing scatter in the values of the temperature gradient is more significant (maximal and minimal values differ by almost a factor of 2); therefore, the absolute value of the temperature gradient significantly influences the composition of gasification products.

In Table 2, ratios between elements for all compositions are also presented. In the case of HMX, the account of diffusion and thermo diffusion resulted in slight improvement in the element balance, and, in the case of RDX, in slight worsening. The maximal deviation of element content from the initial amount in the case of HMX is only 6.5% (for C), and, in the case of RDX, 8.3% (for O). For a mixture of 11 species, this can be regarded as a good agreement with the initial content of elements.

Brutto-reactions of gasification of RDX and HMX at a pressure of 0.1 MPa according to compositions of gasification products from Table 2 are given as:

$$\begin{aligned} \mathrm{RDX} \rightarrow\ & 1.236\ \mathrm{NO} + 0.934\ \mathrm{HCN} + 0.908\ \mathrm{H_2O} + 0.605\ \mathrm{CO} + \\ & + 0.589\ \mathrm{H_2} + 0.444\ \mathrm{NO_2} + 0.\ 377\ \mathrm{RDX_v} + 0.277\ \mathrm{N_2O} + \\ & + 0.133\ \mathrm{CO_2} + 0.056\ \mathrm{CH_2O} + 0.050\ \mathrm{N_2} \end{aligned} \quad (6)$$

$$\begin{aligned} \mathrm{HMX} \rightarrow\ & 1.817\ \mathrm{NO} + 1.103\ \mathrm{H_2O} + 0.919\ \mathrm{CO} + 0.905\ \mathrm{HCN} + \\ & + 0.757\ \mathrm{H_2} + 0.508\ \mathrm{N_2O} + 0.421\ \mathrm{N_2} + 0.345\ \mathrm{HMX_v} + \\ & + 0.309\ \mathrm{NO_2} + 0.240\ \mathrm{CO_2} + 0.298\ \mathrm{CH_2O} \end{aligned} \quad (7)$$

Obtained brutto-reactions for gasification of nitramines represent an averaged picture of decomposition and vaporization processes in the surface layer of the condensed phase.

The heat release in the reaction layer of the condensed phase can be determined using the stoichiometric coefficients of brutto-reaction for gasification (ν_i).

$$Q = -\Delta H_{T=T_s} = H(HMX_l)_{T=T_s} - \sum \nu_i \cdot H(B_i)_{T=T_s} \quad (8)$$

$$H(HMX_l)_{T=T_s} = \Delta_f H^0(HMX_s) + \int_{T_0}^{T_{\beta\rightarrow\delta}} c_{p,\,HMX_\beta}(T)dT + q_{\beta\rightarrow\delta} + \int_{T_{\beta\rightarrow\delta}}^{T_{\delta\rightarrow l}} c_{p,\,HMX_\delta}(T)dT +$$

$$+ q_{\delta\rightarrow l} + \int_{T_{\delta\rightarrow l}}^{T_s} c_{p,\,HMX_l}(T)dT \quad (9)$$

The heat release in the reaction layer of the condensed phase can also be calculated on the basis of consideration of the heat balance on the burning surface.

Comparison of these equations shows that difference between these values (ΔQ) can be expressed by the formula:

$$Q = \int_{T_0}^{T_{\beta\to\delta}} c_{p,\,HMX_\beta}(T)dT + q_{\beta\to\delta} + \int_{T_{\beta\to\delta}}^{T_{\delta\to l}} c_{p,\,HMX\delta}(T)dT + q_{\delta\to l} + \int_{T_{\delta\to l}}^{T_s} c_{p,\,HMXl}(T)dT - q - q_r \qquad (10)$$

$$q = \lambda_g(T)\cdot(dT/dz)_{z=0}/m \qquad (11)$$

$$\Delta Q = \Delta_f H^0(HMX_s) + q + q_r - \sum \nu_i \cdot H(B_i)_{T=T_s} \qquad (12)$$

One can see that ΔQ in comparison with absolute values of Q is determined by less number of parameters. It depends only on the standard enthalpy of formation of the initial compound, the heat feedback from the gas phase to the gas phase and the composition of gasification products.

In the case of HMX, calculations were conducted for three values of T_s and their corresponding values of temperature gradient and mass burning rate. [11,20,24] In the case of RDX, T_s = 600 K was used, and the values of the temperature gradient and mass burning rate were taken from Zenin.[11] Using measured compositions of products near the burning surface, for each value of the burning surface corresponding value of heat conductivity $\lambda_g(T)$ was calculated. Heat feedback to the burning surface by flame radiation, q_r, was neglected because, according to Zenin and Finjakov,[21] it comprises only 7 cal/g in the case of HMX and 6 cal/g in the case of RDX.

Table 3: Difference between values of heat release in reaction layer of the condensed phase (ΔQ), calculated using brutto-reaction of gasification and equation of heat balance on the burning surface

RDX	HMX		
T_s = 600 K,* $dT/dx=8\cdot10^6$ K/m Brill et al.[23]	T_s = 687 K, $dT/dx=3.55\cdot10^6$ K/m Sinditskii et al.[24]	T_s = 633 K, $dT/dx=4\cdot10^6$ K/m Brill et al.[23]	T_s = 593 K, $dT/dx=7\cdot10^6$ K/m Zenin et al.[20]
q = 117 cal/g	q = 121 cal/g	q = 95 cal/g	q = 133 cal/g
ΔQ = 92 cal/g	ΔQ = 123 cal/g	ΔQ = 116 cal/g	ΔQ = 170 cal/g

*Mean value obtained using data of Parr et al.[2] and Zenin[11]

The difference between values of heat release in the reaction layer of the condensed phase, calculated using brutto-reaction of gasification and equation of heat balance on the burning surface, turned out to be quite high (Table 3). This discrepancy is most likely caused by inaccuracy in determining both the

composition of gasification products and the value of heat feedback from gas phase to the condensed phase by heat conductivity (q). Table 3 shows that for HMX, difference in values of q reaches ~ 40 cal/g. The last term in the expression for ΔQ is a sum of positive and negative values close in magnitude, therefore even slight changes in stoichiometric coefficients can result in a significant decrease of ΔQ. In the case of RDX, ΔQ is equal to 92 cal/g. Variation of experimentally-measured composition of products near the burning surface of RDX (within the limits of measurement error) allowed us to obtain a better agreement between the values of heat release calculated using brutto-reaction for gasification and the equation of heat balance. It should be noted that the composition was changed in such a way to simultaneously improve element balance. Concentrations of H_2O and HCN underwent a maximal change ~ 20%. Concentrations of other products were changed by ~ 10%, or not changed at all. In the case of HMX, concentrations of all products found near the burning surface have not been determined, and even all products have not been identified. Therefore, analysis of the variation in the measured composition of products, near the burning surface of HMX, in order to obtain better agreement between values of heat release calculated using brutto-reaction of gasification and equation of heat balance, was not conducted. Some species, concentrations of which have yet to be determined, for example, triazine ($C_3H_3N_3$) and dicyan (C_2N_2), have high positive values of enthalpy formation. An accounting of these species' concentrations can significantly decrease the existing difference in values of Q.

Using data from Table 2, the pressure from RDX and HMX vapor, which formed during gasification in the combustion wave at a pressure of 0.1 MPa, can be calculated. Pressure of RDX vapor comprises 0.067×101325≈6.8 kPa, pressure of HMX vapor, 0.045×101325≈4.6 kPa. These pressures can also be estimated by another method. According to Maksimov[25] vapor pressures over liquid RDX and HMX are given as:

$$P_{RDXv}=10^{12.4\pm1}\exp[-(11300\pm250)/T] \quad (13)$$

$$P_{HMXv}=10^{13.1\pm2}\exp[-(13870\pm500)/T) \quad (14)$$

where P is in Pa, T is in K. At a temperature of $T=T_s=600$ K, the equilibrium vapor pressure for RDX is equal to 16.6 kPa. Using this value and knowing the fraction of RDX transferring from the burning surface to the gas phase as vapor, pressure of forming RDX vapor can be estimated at: 16.6×0.377≈6.3 kPa. This value is in agreement with the above-obtained value of RDX vapor, forming during RDX gasification (6.8 kPa) in the combustion wave. In the case of HMX, the scatter of values in temperature of the burning surface from 593 to 687 K resulted in a range of equilibrium pressures of HMX vapor from 0.9 to 22 kPa. Taking into account the fraction of HMX, transferred from the burning

surface to the gas phase as a vapor (0.345), resulted in a pressure range from 0.3 to 7.6 kPa. The above-obtained value of HMX vapor, formed during HMX gasification in the combustion wave (4.6 kPa), lies within this range. However, this coincidence is most likely accidental. The inaccuracy of parameters in the above-presented equations for the equilibrium vapor pressure of RDX and HMX leads to significant scatter in values of vapor pressure, which are several times higher than absolute values of vapor pressure obtained by MBMS in nitramine flames.

CONCLUSIONS

Using molecular beam mass spectrometry, it was found that RDX and HMX flames at a pressure of 0.1 MPa have two-zone chemical structure. Near the burning surface, a zone of nitramine vapor decomposition was experimentally found. Eleven species, including nitramine vapor (RDX_v or HMX_v), were identified, and their concentrations were measured in the flame of nitramines at a pressure of 0.1 MPa. Using measured compositions of products near the burning surface, brutto-reactions for gasification of nitramines at a pressure of 0.1 MPa were determined. Data obtained in this work can be used for further improvement of combustion mechanisms for nitramines.

REFERENCES

[1]Korobeinichev, O.P., Kuibida, L.V., Paletsky, A.A., and Chernov, A.A. (1996) Study of Solid Propellant Flame Structure by Mass-Spectrometric Sampling, *Comb., Sci. Tech.*. **113–114**:557–71.

[2]Parr, T.P. and Hanson-Parr, D.M. (1996) Solid Propellant Flame Structure, *Proc. Mat. Res. Soc.*, *Vol. 418*, T.B. Brill, T.P. Russell, W.C. Tao, and R.B. Wardle (eds.), Materials Research Society, Pittsburgh, PA.

[3]Lee, Y.J., Tang, C.-J., and Litzinger, T.A. (1999) A Study of the Chemical and Physical Processes Governing CO_2 Laser-Induced Pyrolysis and Combustion of RDX, *Comb. Flame*. **117**:600–28.

[4]Korobeinichev, O.P., Kuibida, L.V., Orlov, V.N., Tereschenko, A.G., Kutsenogii, K.P., Mavliev, R.V., Ermolin, N.E., Fomin, V.M, Emel'yanov, I.D. (1985) Mass-Spectrometric Probe Study of the Flame Structure and Kinetics of Chemical Reactions in Flames, *Mass-Spectrometry and Chemical Kinetics,* V. Tal'roze (ed.), Nauka, Moscow (in Russian).

[5]Korobeinichev, O.P., Kuibida, L.V., and Madirbaev, V.Zh. (1984) Investigation of the Chemical Structure of the HMX Flame, *J. Comb., Expl., Shock Waves*. **20**:282–5

[6]Tang, C.-J., Lee, Y.J., Kudva, G., and Litzinger, T.A. (1999) A Study of the Gas-Phase Chemical Structure During CO_2 Laser Assisted Combustion of HMX *Comb. Flame.* **117**:170–88.

[7]Beckstead, M.W. (2006) Recent Progress in Modeling Solid Propellant Combustion, *Comb., Expl., Shock Waves* **42**:623–41.

[8]Simonenko, V.N., Zarko, V.E., and Kiskin, A.B. (1998) Characterization of Self-Sustain Combustion of Cyclic Nitramines, *Proceedings of the 29th International Annual Conference of* Institut Chemische Technologie, June 30-July 3, Karlsruhe, Federal Republic of Germany, Fraunhofer Institut Chemische Technologie, Karlsruhe.

[9]Trusov, B. (1990) *Multi-Purpose ASTRA Code for Modeling Chemical and Phase Equilibria at High Temperature, ver. 2/24*, Moscow State Technical University, Moscow.

[10]Homan, B.E., Miller, M.S., and Vanderhoff, J.A. (2000) Absorption Diagnostics and Modeling Investigations of RDX Flame Structure. *Comb. Flame* **120**:301–17.

[11]Zenin, A. (1995) HMX and RDX: Combustion Mechanism and Influence on Modern Double-Base Propellant Combustion, *J. Prop. Power* **11**:752–8.

[12]Melius, C.F. (1990) Thermochemical Modeling, II, Application to Ignition and Combustion of Energetic Materials, *Chemistry and Physics of Molecular Processes in Energetic Materials*, S. Bulusu (ed.), Kluwer, Boston.

[13]Yetter, R.A., Dryer, F.L., Allen, M.T., and Gatto, J.L. (1995) Development of Gas-Phase Reaction Mechanisms for Nitramine Combustion, *J. Prop. Power* **11**:683–97.

[14]Liau, Y.-C., and Yang, V. (1995) Analysis of RDX Monopropellant Combustion with Two-Phase Subsurface Reactions, *J. Prop. Power* **11**:729–39.

[15]Prasad, K., Yetter, R.A., and Smooke, M.D. (1997) An Eigenvalue Method for Computing the Burning Rates of RDX Propellants, *Comb., Sci. Tech.* **124**: 35–82.

[16]Davidson, J.E. and Beckstead, M.W. (1997) Improvements to Steady State Combustion Modeling of Cyclotrimethylenetrinitramine, *J. Prop. Power* **13**:375–83.

[17]Liau, Y.C. (1996) A Comprehensive Analysis of RDX Propellant Combustion and Ignition with Two-Phase Subsurface Reactions, Doctorate Dissertation, The Pennsylvania State University, University Park, PA, USA.

[18]Krien, G., Licht, H.H., and Zierath, J. (1973) Thermochemische Untersuchungen an Nitraminen, *Thermochimica Acta* **6**:465–72.

[19]NIST Chemistry WebBook (http://webbook.nist.gov/chemistry/).

[20]Zenin, A.A., Puchkov, V.M., and Finyakov, S.V. (1998) Characteristics of HMX Combustion Waves at Various Pressures and Initial Temperatures, *Comb., Expl. Shock Waves* **34**:170–76.

[21]Zenin, A. and Finjakov, S. (2006) Characteristics of Octogen and Hexogen Combustion: A Comparison, *Proceedings of the 37th International Annual Conference of the Institut Chemische Technologie*, June 27-30, Karlsruhe, Federal Republic of Germany, Fraunhofer Institut Chemische Technologie, Karlsruhe.

[22]Parr, T. and Hanson-Parr, D. (1994) Solid Propellant Flame Chemistry and Structure, *Non-Intrusive Combustion Diagnostics*, K.K. Kuo, and T.P. Parr (eds.), Begell House, New York.

[23]Brill, T.B., Arisawa, H., Brush, P.J., Gongwer, P.E., and Williams, G.K. (1995) Surface Chemistry of Burning Explosives and Propellants, *J. Phys. Chem*. **99**:1384–92.

[24]Sinditskii, V.P., Egorshev, V.Y., and Berezin, M.V. (2001) Study on Combustion of New Energetic Nitramines, *Proceedings of the 32th International Annual Conference of the Institut Chemische Technologie*, July 3-6, Karlsruhe, Federal Republic of Germany, Fraunhofer Institut Chemische Technologie, Karlsruhe.

[25]Maksimov, Y.Y. (1992) Boiling Point and Enthalpy of Evaporation of Liquid Hexogen and Octogen, *Russ. J. Phys. Chem*. **66**:280–1.